Solar Polarization 6
ASP Conference Series, Vol. 437
Kuhn, Berdyugina, Harrington, Keil, Lin, Rimmele, and Trujillo-Bueno, eds.
©2011 Astronomical Society of the Pacific

Polarimetry with GREGOR

H. Balthasar,[1] N. Bello González,[2] M. Collados,[4] C. Denker,[1] A. Feller,[3] A. Hofmann,[1] A. Lagg,[3] K. Nagaraju,[3] K. G. Puschmann,[4,1] D. Soltau,[2] and R. Volkmer[2]

[1]*Astrophysikalisches Institut Potsdam, An der Sternwarte 16, D-14482 Potsdam, Germany*

[2]*Kiepenheuer-Institut für Sonnenphysik, Schöneckstr. 6, D-79104 Freiburg, Germany*

[3]*Max-Planck-Institut für Sonnensystemforschung, Katlenburg-Lindau, Germany*

[4]*Instituto de Astrofísica de Canarias, E-38200 La Laguna, Tenerife, Spain*

Abstract. A brief description of the new 1.5-meter solar telescope GREGOR located at the Observatorio del Teide in Tenerife will be given. GREGOR will provide a spatial resolution of about 75 km on the Sun, and with its light collecting capability we will be able to study the development of small magnetic features with high cadence. From the beginning, it will be equipped with the GREGOR Fabry-Pérot Interferometer (GFPI) for the visible spectral range and with a GRating Infrared Spectrograph (GRIS). Both postfocus instruments can be combined with a polarimeter, and in both cases the light is modulated by two ferro-electric liquid crystals. A calibration unit can be inserted to determine the instrumental polarization. Because of the altazimuthal mount, time-dependent rotation of the polarimetric reference plane is introduced, and we have to develop a polarization model of the telescope. Measurements to verify this model are in preparation.

1. Introduction

A new generation of groundbased solar telescopes is presently under development or already under construction. These instruments will be able to resolve solar structures much smaller than 100 km on the Sun, what is very important to understand the small scale structures of the solar magnetic field. Among these telescopes are the New Solar Telescope at Big Bear Solar Observatory (NST, Goode 2010), the Advanced Solar Telescope (ATST, Keil 2010), the European Solar Telescope (EST, Bettonvil 2010), and GREGOR (Volkmer et al. 2010).

GREGOR is a solar telescope with an aperture of 1.5 m presently under construction in the Observatorio del Teide on the island of Tenerife (Spain). A consortium of three German institutes, the Kiepenheuer-Institut für Sonnenphysik Freiburg, the Universität Göttingen, and the Astrophysikalisches Institut Potsdam, was founded in 2002

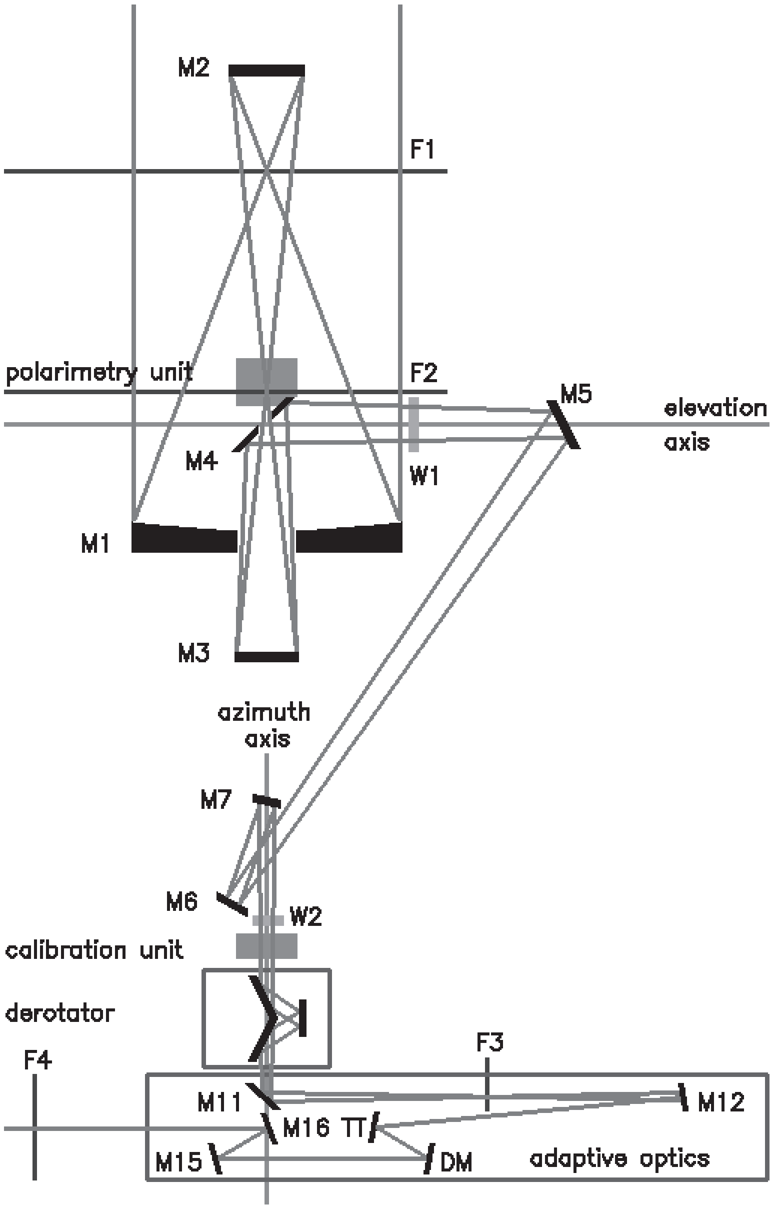

Figure 1. Sketch of the optical path of the GREGOR telescope. Mirrors are indicated by M1 – M16, focal planes by F1 – F4, and windows of the coudé train by W1 and W2. TT and DM are the tip-tilt and deformable mirror of the AO system.

to build the new telescope. In 2008, the Universität Göttingen was replaced by the Max-Planck-Institut für Sonnensystemforschung in Katlenburg-Lindau. Major international contributions were provided by the Astronomical Institute Ondřejov (Czech Republic) and by the Instituto de Astrofísica de Canarias (Spain). A description of the telescope is given by Balthasar et al. (2007) and Volkmer et al. (2010). GREGOR will be able to resolve solar fine structures of about 50 – 75 km.

To avoid heating at critical locations inside the telescope, GREGOR is an open construction, so that ambient air flows through it, thus carrying the heat away from the optical surfaces. In addition, precooled air is blown onto the backside of the main mirror M1. M1 is made from a light-weighted Zerodur blank and will be delivered in fall 2010. Temperature differences between the optical surface of M1 and the ambient air will be kept below 1°C. For early commissioning, a smaller mirror with a diameter of 1 m on loan from the SolarLite project was inserted in 2009 and will remain until the final M1 is ready. In the primary focus is a watercooled fieldstop with a default diameter of 150″. The rest of the light is reflected out of the telescope.

The light is then transferred by two elliptical mirrors M2 and M3 to the tertiary focus. These two mirrors are made from Cesic, a material with high thermal conductivity guaranteeing low temperature differences to the ambience. The properties of this material would be excellent also for M1, but so far, no blank with 1.5 m diameter could be successfully produced. A series of plane mirrors deflect the light through elevation and azimuth axes towards F3. The coudé train (mirrors M5 – M7) is enclosed by two glass plates and can be evacuated to avoid turbulent air next to the pupil image and a chimney effect. To compensate the image rotation, a derotator can be inserted behind the coudé train. After F3 the light passes the adaptive optics (AO) system (see Berkefeld et al. 2006) and is finally distributed to the postfocus instruments. A sketch of the light path is given in Fig 1.

2. The GREGOR Polarimetry Unit

Polarimetric measurements need instrumental calibration. For this purpose, the GREGOR Polarimetry Unit (GPU Hofmann et al. 2009) will be inserted next to the secondary focus F2. It consists of two revolving wheels. For normal observations, open apertures on both wheels let the light pass. Besides three presently open apertures, the first wheel carries a linear polarizer, which is a Marple-Hess prism. It can be used for the spectral range 350 – 2000 nm. The linear polarizer is pivoted on the wheel and can be rotated with a position accuracy of $0\overset{\circ}{.}1$. The second wheel is located exactly in the focal plane. Two achromatic quarter wave plates, one for the visible and one for the near infrared light, are mounted on this wheel. Both are made from polymethylmetacrylat. They are designed as superachromatic retarders for the ranges 380 – 800 nm and 750 – 1800 nm, respectively. They can be alternately inserted into the light beam. These retarders too can be rotated in small steps. In addition, this wheel contains a target grid and a pinhole for adjustment purposes. The light beam can be blocked for dark exposures. The GPU was tested at the Einsteintower in Potsdam, and its high efficiency is demonstrated by Hofmann et al. (2009). Figure 2 shows the GPU inserted in the GREGOR telescope.

Inserting the linear polarizer and one of the two retarders into the optical beam, a variety of polarization states can be produced, and polarizing properties of the optical

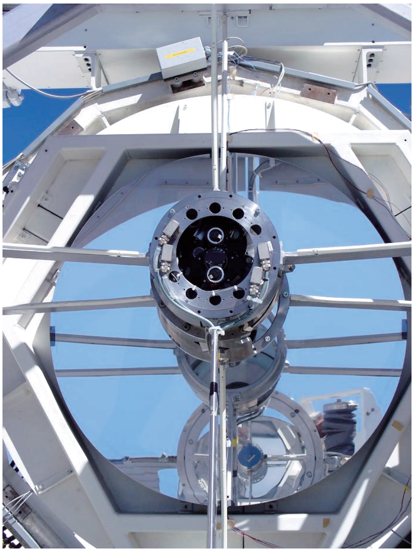

Figure 2. The GPU inserted in the telescope. In this position, the light coming from the secondary mirror passes the linear polarizer in the center of GPU. Behind the GPU, the preliminary 1-m SolarLite mirror is seen.

elements between F2 and the detector of the postfocus instrument can be calibrated. Since the beam is axisymmetric before F2, the instrumental polarization from M1 and M2 is very small (the instrument is free of polarization at the 10^{-4} level) and can be neglected.

However, the angles between the mirrors after M3 change with time depending on azimuth and elevation of the telescope. When the image rotation is compensated by the derotator, this also introduces time-dependent instrumental polarization. To disentangle effects of the telescope itself and the following instruments, it is planned to insert a second calibration unit between the exit window of the coudé train and the derotator. Instrumental polarization originating behind the derotator is not time-dependent during a measurement. Measurements with the second calibration unit will be taken with and without derotator.

3. Polarimetric Telescope Model

The angles in the telescope might change rather rapidly, and it is not sufficient to calibrate the telescope by measuring the instrumental calibration before or after the scientific measurement. A telescope model is needed. For this purpose, we follow the principles described by Beck et al. (2005). We calculate the Mueller matrices of the mirrors, which are all coated with aluminum until M11. Then we have to consider the rotation of the reference planes. At F2, this reference plane is the elevation plane. Following the definition of Capitani et al. (1989), the reference frame at a certain mirror is given by the plane of incident and reflected beam. We still have to determine the influence of the windows of the coudé train, but it should be possible to treat them, too. Finally, all these matrices have to be multiplied.

$$M_{\mathrm{GRE}} = PF \cdot AO \cdot M11 \cdot R10 \cdot D \cdot R7 \cdot W2 \cdot M7 \cdot M6 \cdot M5 \cdot R5 \cdot W1 \cdot M4 \cdot R4 \cdot M3 \cdot M2 \cdot M1 \cdot R1$$

Mueller matrices of the mirrors are indicated by M, rotation matrices by R, D denotes the derotator which can be omitted in the calculation, $W1$ and $W2$ stand for the coudé train windows and AO and PF for the influence of the AO-system and the postfocus instruments. Rotation $R1$ changes from the solar North-South reference plane to the elevation plane.

The code is written in IDL. Keywords allow to skip in the calculation special parts of the optical beam. The code will be verified during the commissioning phase of GREGOR. After that it will become part of the data reduction package for GREGOR.

4. Postfocus Instruments

With begin of scientific operations, GREGOR will be equipped with two postfocus instruments. One is the GRating Infrared Spectrograph (GRIS, Collados et al. 2008), which is optimized for the near infrared range. It will be combined with the Tenerife Infrared Polarimeter 2 (TIP 2, Collados et al. 2007). The other one is a two-dimensional spectrometer, the GREGOR Fabry-Pérot Interferometer (GFPI, Denker et al. 2010). A polarimeter can be inserted in GFPI, too.

4.1. The Grating Infrared Spectrograph

The GRIS is a classical slit spectrograph. Its heart is a grating with 316 grooves per millimeter and a Blaze angle of $63\overset{\circ}{.}5$. Both, collimator and camera mirror have a diameter of 35 cm and a focal length of 6 m. This leads to a linear dispersion well adapted to the pixel size of an infrared detector. In principle, however, the spectrograph can also be used in the visible. This spectrograph has a theoretical resolving power of $\mathcal{R} \approx 525,000$ at 1100 nm.

For polarimetry, GRIS can be combined with TIP 2, an upgrade of the polarimeter TIP, which was successfully used since 1999 at the Vacuum Tower Telescope (VTT) on Tenerife. TIP 2 consists of two ferro-electric liquid crystal retarders (FLCR) and a polarizing beam splitter. Two pairs of FLCRs are available, one is optimized for 1564.8 nm, where a neutral iron line with a Zeeman-splitting factor of 3.0 is present, the other pair is centred on the Helium line at 1083 nm. The HgCdTe detector has 1024 $\times$ 1020 pixels, and the pixel size is 18 μm. The chip is placed inside a dewar where it is cooled by liquid nitrogen.

Since FLCRs can be switched only between two states corresponding to a rotation of the fast axis by 45°, only linear combinations of the Stokes parameters can be recorded. Four measurements for the four possibilities of the FLCRs will be taken. Knowing the instrumental calibration, this system of linear equations can be solved, and the observations can be demodulated.

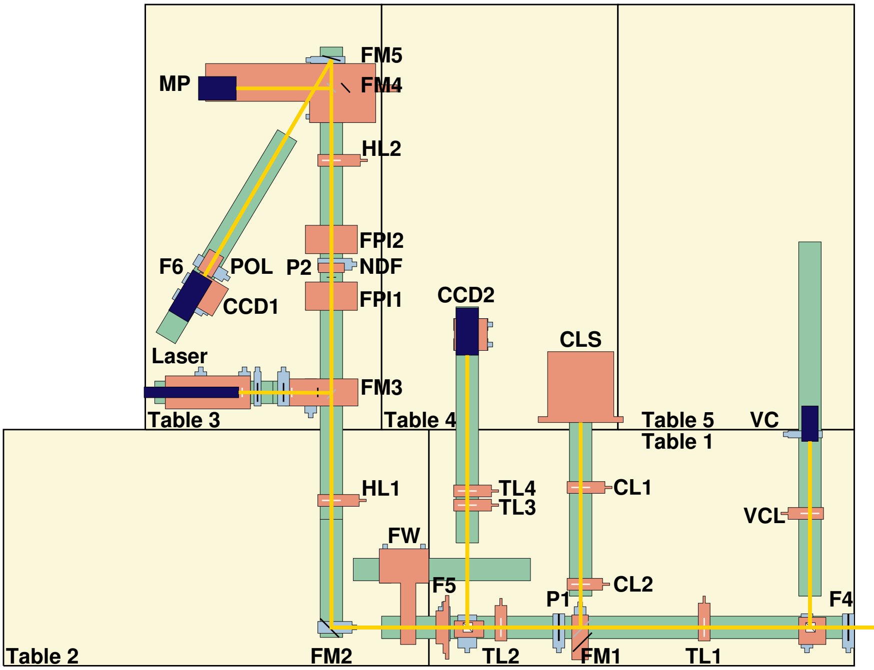

Figure 3. The optical layout of GFPI. Light enters from the lower right at F4. Blue light is then deflected to the video channel (VC). Continuum light can be inserted at FM1. A small fraction of light is sent into the broadband channel (CCD2). The main beam passes a wheel carrying narrowband filters (FW) and then reaches the FPIs. Finally, folding mirror FM5 sends the light to CCD1. Laser light can be inserted at FM3 to align the etalons.

4.2. The GREGOR Fabry-Pérot Interferometer

The GREGOR Fabry-Pérot Interferometer (GFPI) is an upgrade of the Göttingen Fabry-Pérot interferometer which was successfully operated for many years at the VTT on Tenerife. The modifications are described by Puschmann et al. (2006, 2007).

The core of GFPI is formed by two Fabry-Pérot etalons with spacings of 1.101 mm and 1.408 mm and a free aperture of 70 mm. The optical setup of GFPI is shown in Fig. 3. The position of the FPIs is close to the pupil image P2 in the collimated beam. The FPIs step in spectral direction delivering a scan along a spectral line. The spectral resolving power is $\mathcal{R} \approx 250,000$. An image is obtained at each wavelength step. To separate the orders of the FPIs, a narrow (0.3 – 0.5 nm) interference filter is mounted on a filter wheel and can be exchanged to switch the wavelength range. Part of the light is taken out from the main optical beam to record simultaneous broadband images in a fixed wavelength range, unchanged during the stepping of the FPIs. These images are used to correct for the remaining seeing effects. A sufficiently high number of images allows a speckle reconstruction which can be used to deconvolve the narrowband images (Bello González & Kneer 2008).

The combined transmission curve of the FPIs and the interference filter can be measured when artificial continuum light is inserted via FM1. For alignment of the etalons, laser light can be inserted just before the FPIs using FM3. The coatings of the FPIs have a sufficiently high reflectivity in the range 530 – 860 nm. Light shorter than 500 nm is deflected to the video channel and can be used for live images or independent exposures.

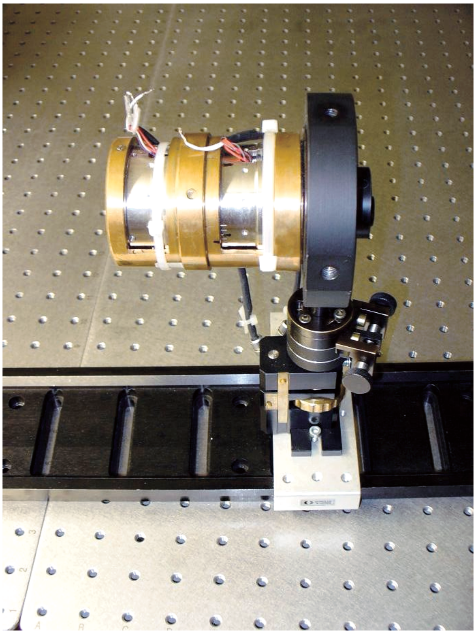

Figure 4. The GFPI polarimeter. It contains the two liquid crystals in the brass-colored part and the modified Savart plate in the black part.

A polarimeter can be inserted just in front of the detector in the narrowband beam. This polarimeter consists of two FLCRs and a modified Savart-plate. The first liquid crystal acts at 630 nm as halfwave plate and the second one as quarterwave plate. The modified Savart plate is build up from two polarizing beam splitters and another halfwave plate which exchanges the ordinary and the extraordinary beam. The separation of the two beams is optimized this way, and the orientation of the astigmatism is the same and can be corrected by inserting a cylindrical lense. The polarimeter is shown in Fig. 4. The present set of FLCRs yields good efficiencies for the spectral range 580 – 660 nm. Details of the polarimeter and an application are presented by Bello González & Kneer (2008).

5. Conclusions

GREGOR will be the most powerful solar telescope for several years until the ATST comes into operation. In the beginning, GREGOR will be equipped with two sophisticated spectropolarimetric instruments, GRIS and GFPI. Instrumental polarization will be measured, and a telescope model is prepared, so that polarimetric measurements can be properly calibrated. More postfocus instruments will be added in the future.

References

Balthasar, H., von der Lühe, O., Kneer, F., Staude, J., Volkmer, R., Berkefeld, T., Caligari, P., Collados, M., Halbgewachs, C., Heidecke, F., Hofmann, A., Klvaňa, M., Nicklas, H., Popow, E., Puschmann, K., Schmidt, W., Sobotka, M., Soltau, D., Strassmeier, K., & Wittmann, A. 2007, in The Physics of Chromospheric Plasmas, edited by P. Heinzel, I. Dorotovič, & R. J. Rutten (San Francisco: Astronomical Society of the Pacific), vol. 368 of ASP Conf. Series., 605

Beck, C., Schlichenmaier, R., Collados, M., Bellot Rubio, L., & Kentischer, T. 2005, A&A, 443, 1047

Bello González, N., & Kneer, F. 2008, A&A, 480, 265

Berkefeld, T., Soltau, D., & von der Lühe, O. 2006, Proc SPIE, 6272, 627205

Bettonvil, F. 2010, in 6^{th} Solar Polariization Workshop, edited by J. Kuhn, H. Lin, & S. V. Berdyugina (San Francisco: Astronomical Society of the Pacific), vol. THISONE of ASP Conf. Series., 9999

Capitani, C., Cavallini, G., Ceppatelli, G., Landi degl Innocenti, E., Landi degl Innocenti, M., Landolfi, M., & Righini, A. 1989, Solar Phys., 120, 173

Collados, M., Calcines, A., Díaz, J. J., Hernández, E., López, R., & Páez, E. 2008, Proc SPIE, 7014, 70145Z

Collados, M., Lagg, A., Díaz Garcíia, J. J., Hernández Suárez, E., López López, R., Páez Maña, E., & Solanki, S. K. 2007, in The Physics of Chromospheric Plasmas, edited by P. Heinzel, I. Dorotovič, & R. J. Rutten (San Francisco: Astronomical Society of the Pacific), vol. 368 of ASP Conf. Series., 611

Denker, C., Balthasar, H., Hofmann, A., Bello González, N., & Volkmer, R. 2010, Proc SPIE, 7735, 245

Goode, P. 2010, in 6^{th} Solar Polariization Workshop, edited by J. Kuhn, H. Lin, & S. V. Berdyugina (San Francisco: Astronomical Society of the Pacific), vol. THISONE of ASP Conf. Series., 9999

Hofmann, A., Rendtel, J., & Arlt, K. 2009, Centr. Eur. Astrophys. Bull., 33, 317

Keil, S. 2010, in 6^{th} Solar Polariization Workshop, edited by J. Kuhn, H. Lin, & S. V. Berdyugina (San Francisco: Astronomical Society of the Pacific), vol. THISONE of ASP Conf. Series., 9999

Puschmann, K. G., Kneer, F., Nicklas, H., & Wittmann, A. D. 2007, in Modern Solar Facilities – Advances in Solar Science, edited by F. Kneer, K. G. Puschmann, & A. D. Wittmann (Göttingen: Universitätsverlag Göttingen), 45

Puschmann, K. G., Kneer, F., Seelemann, T., & Wittmann, A. D. 2006, A&A, 451, 1151

Volkmer, R., von der Lühe, O., Denker, C., Solanki, S. K., Balthasar, H., Berkefeld, T., Caligari, P., Collados, M., Fischer, A., Halbgewachs, C., Heidecke, F., Hofmann, A., Klvaňa, M., Kneer, F., Lagg, A., Popow, E., Schmidt, D., Schmidt, W., Sobotka, M., Soltau, D., & Strassmeier, K. 2010, AN, 331, 624